Spectrometric fluorescence and Raman lidar at ARTE site for advanced tropospheric studies

G. Giuliano[(a)], G. L. Liberti[(a)], M. Di Paolantonio[(a)], L. Masi[(a, b)], and D. Dionisi[(a)]
[(a)] Italian National Research Council, Institute of Marine Sciences, (CNR-ISMAR), 00133 Rome, Italy
[(b)] "Parthenope" University of Naples, 80133 Naples, Italy
Lead Author e-mail address: giovanni.giuliano@cnr.it

Abstract: A multi-grating, 32-channel spectroscopic system has been recently integrated into the multi-telescope Rayleigh–Mie–Raman (RMR) lidar system at the Italian National Facilities Atmospheric Rome joinT SupersitE (ARTE-NF) in Rome Tor Vergata (CNR). Preliminary results on examples of potential atmospheric research applications are reported. The enhanced spectrometric fluorescence and Raman lidar is designed to improve the system's capability to characterize atmospheric constituents with higher spectral resolution and channel diversity, thereby supporting the detection of aerosol fluorescence, atmospheric water vapor and CO_2 mixing ratio. These advancements in lidar technology contribute to a more detailed understanding of aerosol and atmospheric trace gases. Such improvements are crucial for enhancing the reliability of atmospheric monitoring systems and for refining models that predict aerosol impacts on climate, air quality, and human health.

1. Introduction

In recent years, the application of spectroscopic lidar systems for the characterization of atmospheric aerosols has seen significant advancements. These developments have been driven by the implementation of several innovative techniques, including the use of multiple dedicated channels equipped with interference filters [1]. This approach allows for enhanced spectral resolution, enabling more precise differentiation of aerosol types and their optical properties. In parallel, the integration of multi-anode photomultiplier tubes (PMTs) with spectrometers has emerged as another powerful methodology for aerosol analysis, as demonstrated in the work of Reichardt et al. [2] and Yadav et al. [3]. This combination facilitates the simultaneous collection of a broader range of wavelengths, improving the profiling capability of characterizing aerosols and atmospheric trace gases.

2. Experimental setup

The receiving block of the spectrometric fluorescence and Raman lidar system developed at ARTE NF is shown in Figure 1. The emission block, not shown in the picture, consists of a Nd:YAG laser operating at 354.72 nm (Continuum Powerlite DLS8010, repetition rate 10 Hz, pulse width 5-7 ns). The laser beam is collimated with a 5x beam expander and projected vertically by a computer-controlled motorized fold mirror. The receiving block is equipped with a single f/3.0 Newtonian telescope with a diameter of 500 mm. This large aperture allows for efficient collection of scattered light from the atmosphere, improving the lidar's sensitivity and range for both fluorescence and Raman scattering measurements.

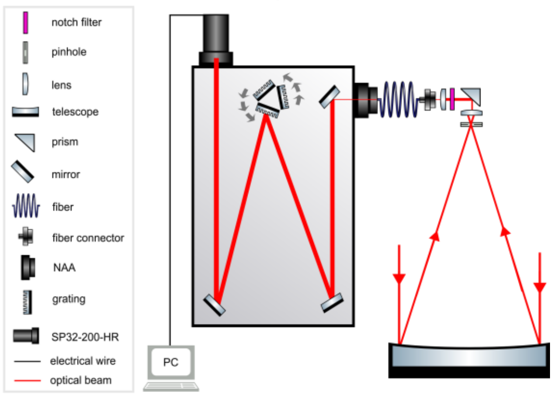

Figure 1. Block diagram of the receiving module of the spectrometric fluorescence and Raman lidar.

The incoming light is directed through a fibre-coupling unit that features a broadband anti-reflection coated right-angle prism. Additionally, a 355 nm blocking notch filter with a full width at half maximum (FWHM) of 26 nm and an average optical density (OD) of 6 is incorporated into this unit to block any unwanted large signal from the primary laser emission, thereby enhancing the signal-to-noise ratio in the collected data. The fiber bundle is connected, at the entrance of the spectrometer, to a numerical-aperture adaptor (NAA) which was designed by Licel so that the optical signals are efficiently transmitted to the detection system with minimal losses. The spectrometer is the Andor Shamrock SR-750, which has a focal length of 750 mm and an f/9.7 optical configuration. The spectrometer is equipped with a motorized triple grating turret, enabling the selection of different diffraction gratings to cover a wide range of spectral regions and resolution. This flexibility is critical for adapting the system to different measurement requirements and optimizing spectral resolution for various atmospheric constituents. The detection part is a single-photon counting system (Licel SP32-200-HR), based on a multi-anode PMT, which is optimized for high-sensitivity photon detection. The high temporal resolution of the system facilitates the detection of fast atmospheric dynamics with a vertical resolution of 7.5 m. Table 1 provides an overview of the spectral ranges covered by the three gratings installed on the system.

Table 1. Gratings specifications.

# (l/mm)		Blaze (nm)	Dispersion (nm/mm)	CWL (nm)	Range (nm)
1	150	500	8.75	496.0	360.4-631.6
2	1200	400	1.04	397.6	381.5-413.7
3	2400	400	0.46	376.9	369.8-384.1

The first grating, with a wide bandpass range, is primarily used for aerosol fluorescence measurements. This allows for the detection and characterization of various aerosol types, such as soot, dust, and organic particles, by exploiting their fluorescence properties. The remaining two gratings, with narrower nominal dispersions, are tailored for the retrieval of atmospheric trace gas concentrations. Grating 2 and grating 3 are optimized for the detection of specific molecular Raman scattering signals, allowing for the accurate determination of mixing ratios of key trace gases such as water vapor (WV) and carbon dioxide (CO_2). These measurements are essential for understanding the role of aerosols and gases in climate processes, atmospheric chemistry, and air quality studies.

3. Pre-processed spectra

The raw data have been processed to account for the pulse pileup [4], background-subtracted, range-corrected, and two-way transmission-corrected for molecular scattering extinction using radiosonde data from the World Meteorological Organization (WMO) station 16245 (LIRE Pratica di Mare) located about 25 km southwest of ARTE [5]. Examples of the acquired signal for the 32 channels for each grating are given in the next section, with a temporal integration over the entire session and a vertical integration from 1 to 5 km. The results reported are preliminary: spectral and radiometric calibrations are yet to be implemented. All contour plots use a perceptually uniform and ordered colour map [6].

4. Preliminary products

An example of aerosol fluorescence profile measurement with grating 1 (150 lines/mm) is given in Figure 2 for a session acquired between 21:00 and 23:30 UTC on the night of 7 August 2025. The dashed black line in top panel indicates the Raman line used for calibration, i.e. N_2 at 386.69 nm. Similarly, the dashed red line shows the position of the WV signal which is expected to be at 407.54 nm.

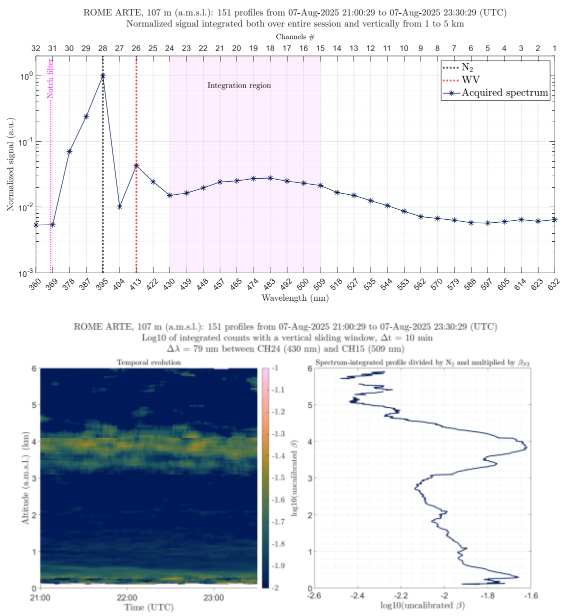

Figure 2. (top) Vertically and spatially integrated spectrum with grating 1 (150 lines/mm). (bottom) Spectrum-integrated temporal evolution between 430 and 509 nm.

An example of water vapor mixing ratio (WVMR) retrieval for the same session as above with grating 1 (150 lines/mm) is shown in Figure 3. The top left panel shows the temporal evolution of the retrieved WVMR also smoothed with a height-dependent sliding average [7]. A cross-comparison with the radiosonde data is given on the top right. The calibration coefficient *C* was calculated in the region between 1.6 km and 2.2 km and a comparison between the radio-sounding profile and the calibrated profile retrieved with the spectrometric Raman lidar is shown in the top right panel. The bottom panels show the relative differences over the range both between ground level up to 6 km and within the selected calibration region. The vertical lines represent the ± 1, 2 and 3 standard deviations.

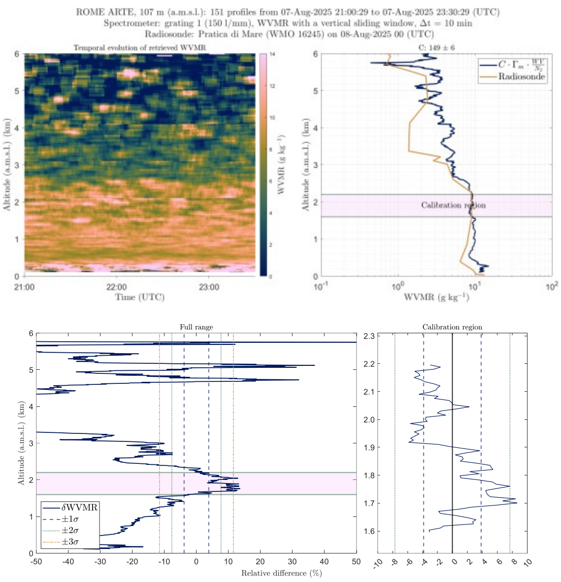

Figure 3. WVMR retrieval with grating 1.

The same WVMR analysis was carried out on a different nighttime session (18:30-23:30 UTC on 10 November 2025) acquired with the higher resolution grating 2 (1200 lines/mm) and it is given in Figure 4. The top panel also shows the simulated Raman lines (CO_2 concentration 425 ppm, WV concentration 1 g/kg) normalized by the maximum intensity within the wavelength range covered by the grating. The solid green line represents these Raman lines integrated over each of the 32 channels in the spectroscopic system with the grating specifications in use as indicated in Table 1. The dashed black and red lines are the same as for grating 1.

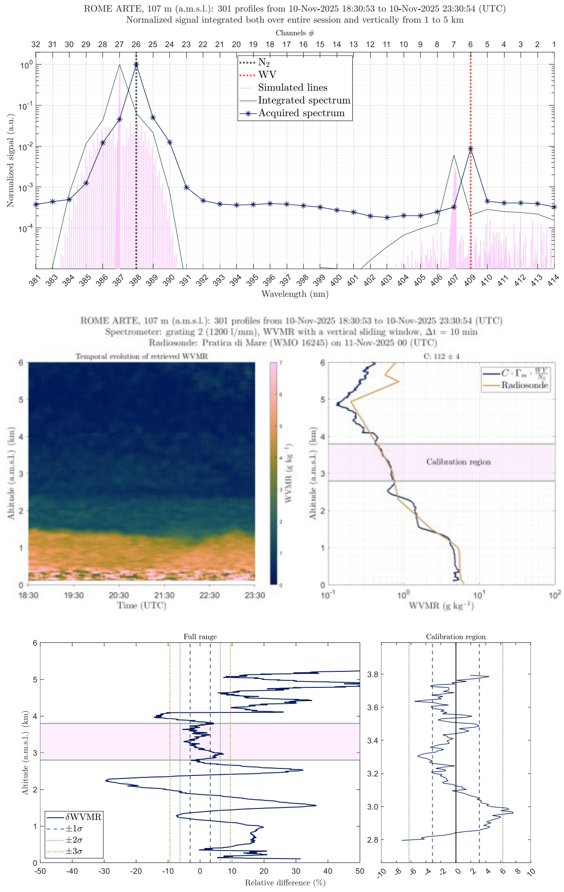

Figure 4. (top) Vertically and spatially integrated spectrum with grating 2 (1200 lines/mm). (center-bottom) WVMR retrieval.

The performance difference in terms of SNR and resolution between the first and second grating is evident, as expected by the grating specifications summarized in Table 1.

To test the capabilities of the novel spectrometric fluorescence and Raman lidar in the context of carbon dioxide retrieval, an example of vertically and temporally integrated spectrum is given in Figure 5 for the nighttime session between 5 December 18:27 and 6 December 2025 03:02 UTC. The dashed black line in the top panel indicates the O_2 roto-vibrational Q-branch Raman line at 375.44 nm used for calibration. Similarly, the dashed red line shows the position of the CO_2 signal which is expected to be at 371.70 nm. The measured peaks of CO_2 and O_2 are clearly visible as confirmed by the theoretical curve [9]. To characterize the feasibility of the CO_2 retrieval with this grating, further investigations are needed specifically focused on: the O_2 ro-vibrational signal leaking into the CO_2 band, the possible stray light due to the strong elastic and/or O_2 Q-branch return signal, optimization of the spectrometer CWL and development of a calibration methodology for CO_2 detection.

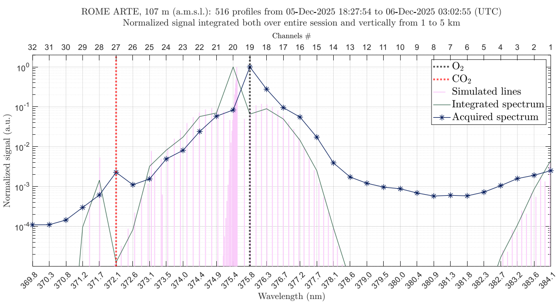

Figure 5. Vertically and spatially integrated spectrum with grating 3 (2400 lines/mm). The CO_2 peak in the acquired signal is marked with a dashed red line.

5. Conclusions

The combination of these advanced components enables the lidar system to offer comprehensive, high-resolution profiling of both aerosols and atmospheric gases, making it a valuable tool for atmospheric monitoring and research. Robust radiometric and spectral calibration will be implemented according to previous works available in this research field with similar experimental setups to the one presented in this study [2-3, 8].

6. Acknowledgments

This project was supported by IR0000032 – ITINERIS, Italian Integrated Environmental Research Infrastructures System (D.D. n. 130/2022 - CUP B53C22002150006) Funded by EU - Next Generation EU PNRR- Mission 4 “Education and Research” - Component 2: “From research to business” - Investment 3.1: “Fund for the realisation of an integrated system of research and innovation infrastructures”

7. References

[1] I. Veselovskii *et al.*, “Multiwavelength fluorescence lidar observations of smoke plumes”, AMT **16**, 2055-2065 (2023).

[2] J. Reichardt, O. Behrendt and F. Lauermann, “Spectrometric fluorescence and Raman lidar: absolute calibration of aerosol fluorescence spectra and fluorescence correction of humidity”, AMT **16**, 1–13 (2023).

[3] A. C. Yadav *et al.*, “Characterizing the Saharan dust transported to the UK through lidar ratio, particle depolarization, and spectroscopic measurements”, Atmos. Environ. **363**, 121613 (2025).

[4] D. P. Donovan, J. A. Whiteway, and A. I. Carswell, "Correction for nonlinear photon-counting effects in lidar systems," Appl. Opt. **32**, 6742-6753 (1993).

[5] B. A. Bodhaine, N. B. Wood, E. G. Dutton and J. R. Slusser, “On Rayleigh Optical Depth Calculations”, JTECH **16**, 1854-1861 (1999).

[6] F. Crameri, G. E. Shephard and P. J. Heron, “The misuse of colour in science communication”, Nat. Commun. **11**, 5444 (2020).

[7] D. N. Whiteman *et al.*, “Demonstration Measurements of Water Vapor, Cirrus Clouds, and Carbon Dioxide Using a High-Performance Raman Lidar”, JTECH **24**, 1377-1388 (2007).

[8] J. Reichardt, “Cloud and Aerosol Spectroscopy with Raman Lidar”, JTECH **31**, 1946-1963 (2014).

[9] M. Di Paolantonio, “Development of a versatile ground-based UV lidar prototype, featuring a CO2 Raman channel, in support of the ASI-NASA CALIGOLA mission”, PhD thesis, Università degli studi della Basilicata (2025).